Spectrochimica Acta Part A: Molecular and Biomolecular Spectroscopy 222 (2019) 117268

Contents lists available at ScienceDirect

Spectrochimica Acta Part A: Molecular and Biomolecular Spectroscopy

journal homepage: www.elsevier.com/locate/saa

Short Communication

Measurement of OH radicals distribution in a microwave plasma sheet using LIF method

Mateusz Tański [a], Marek Kocik [a], Bartosz Hrycak [a], Dariusz Czylkowski [a,*], Mariusz Jasiński [a], Toshiyuki Kawasaki [b], Seiji Kanazawa [c]

[a] Institute of Fluid Flow Machinery, Polish Academy of Sciences, Fiszera 14, 80-231 Gdańsk, Poland
[b] Department of Electrical Engineering, Nishinippon Institute of Technology, 1-11 Aratsu, Kanda, Fukuoka 800-0394, Japan
[c] Faculty of Science and Technology, Oita University, 700 Dannoharu, Oita 870-1192, Japan

ARTICLE INFO

Article history:
Received 11 February 2019
Received in revised form 6 June 2019
Accepted 9 June 2019
Available online 13 June 2019

Keywords:
Microwave plasma
Atmospheric pressure plasma
Plasma sheet
LIF method
OH radicals

ABSTRACT

Microwave plasma sources (MPSs) operating at atmospheric pressure provide plasmas in the form of a flame or cylindrical column. In contrast, this article presents an innovative MPS (patented by us) for generating a new type of plasma, i.e. in the form of a plasma sheet, which is generated in a flat cuboidal quartz box. It is based on a WR 340 waveguide, powered by microwaves of 2.45 GHz and operated in argon at atmospheric pressure. The plasma sheet contains a multitude of filaments typical of microwave argon plasmas. In the presented experiment, the spatial distribution of the OH radicals in the microwave plasma sheet was measured by means of the LIF method. Studies have shown that the relative concentration of OH radicals increases with the increase in microwave power and decreases with the increasing argon flow rate.

1. Introduction

Microwave plasmas that are generated by delivering microwave power for gas ionisation the advantage that they usually do not require the use of electrodes, which in turn eliminates problems associated with electrode degradation. The MPS presented in this article has been patented by us [1]. The overall characteristics of this device have recently been presented by us in [2]. The generated plasma is in the form of a sheet, and this shape is convenient in the surface treatment of materials and the treatment of biological material. In applications including, among others, hydrophilisation, hydrophobisation, graftability, adhesability, printability and surface sterilisation, the key role of OH radicals produced by plasma is evident [3]. Therefore, monitoring OH production during the plasma treatment is important.

Up to now, various methods have been applied for the investigation of OH radicals [4–16]. These methods include optical emission spectroscopy (OES) [4,5], absorption spectroscopy (AS) [6–8], laser-induced fluorescence (LIF) [9,10], electron spin resonance (ESR) [11,12], mass spectrometry (MS) [13] and the chemical probe method (CP) [10,14–16]. Among the methods used for OH monitoring, it is laser-induced fluorescence (LIF) that has shown to have higher sensitivity and selectivity than other methods [17].

The LIF technique in the monitoring of OH radicals has been used for various types of plasmas, e.g. for an RF plasma jet in Ar [18,19], a nanosecond pulsed filamentary discharge in Ne [20], and a DC positive corona discharge in air [21].

As our device generates a new type of plasma, its properties are still poorly understood. The LIF diagnostic investigations of our new plasma type are justified because they belong to the first ones concerning this research object.

2. Measuring method

The LIF method for measuring the concentration of a given gaseous species consists of the excitation of this species using laser radiation and afterwards in measuring the intensity of the fluorescence radiation induced by the laser radiation [22]. Usually the laser induced fluorescence is comprised of the emission of several spectral lines that are characteristic of a particular species. The intensities of the induced characteristic lines are proportional to the concentration of the species. In order to excite a given molecule in the selected quantum state to a higher energy state by laser radiation, the radiation frequency has to be tuned to the quantum transition between those two states. Since generally there are only several laser lines that excite a given molecule and induce its fluorescence, and only several corresponding emission spectral lines, usually the set of these lines enables a molecule to be identified, even in a complex gas mixture.

* Corresponding author.
E-mail address: dczylkowski@imp.gda.pl (D. Czylkowski).

https://doi.org/10.1016/j.saa.2019.117268
1386-1425/

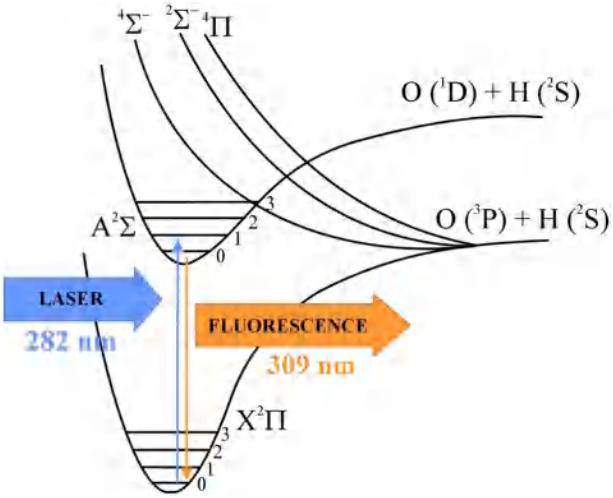

Fig. 1. Energy level diagram of the OH radical.

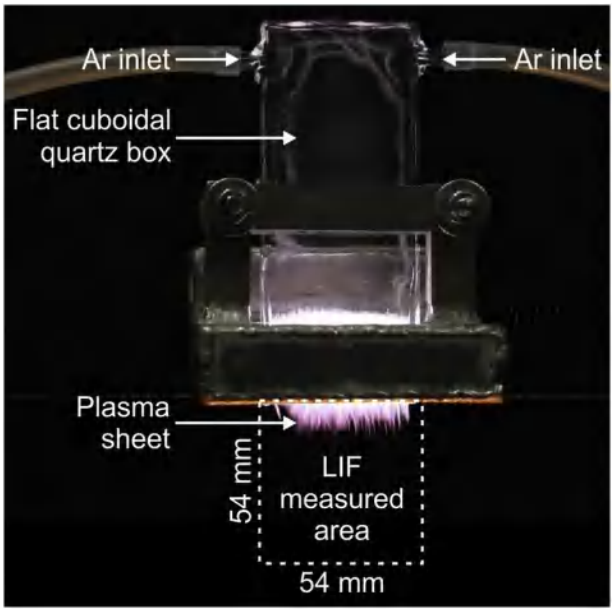

Fig. 3. A picture of the main part of the MPS with the microwave plasma sheet generated in atmospheric pressure argon. Argon flow rate - 20 L/min^{-1}, microwave power - 850 W.

In this experiment, the relative concentration and spatial distribution of the OH radicals in the microwave plasma sheet was measured by means of the LIF method. The method is based on the selective excitation of the OH radicals (Fig. 1) from the rotational-vibrational $X^2\Pi(v'' = 0)$ to states in the rotational-vibrational band $A^2\Sigma^+(v' = 1)$ by a laser line around the wavelength of $\lambda = 282$ nm. Before the LIF measurement was performed, the LIF spectrum (LIF signal vs excitation wavelength) was taken and compared to a simulation from LIFBASE. Thus, all vibrational states around 282 nm were identified as was described in [23]. For this experiment, the transition $Q_1(1) + Q_{21}(1)$ (281.92 nm) was chosen due to it having the strongest fluorescence signal. The LIF signal was observed at around 309 nm [$A^2\Sigma + (v' = 0) \rightarrow X^2\Pi(v'' = 0)$] [9,10].

3. Experimental setup

This chapter has been divided into two sections. The first section (Section 3.1) presents and describes the general experimental setup, which includes the devices necessary to generate a microwave plasma sheet and auxiliary devices. Also, a picture of the actual microwave plasma sheet generated in the experiment is shown. The second section (Section 3.2) presents the experimental setup for the OH LIF measurement.

3.1. Experimental setup for plasma sheet generation

The general scheme of the experimental setup with the microwave plasma source (MPS) for the plasma sheet generation is shown in Fig. 2. The main part of the MPS with generated plasma is shown in Fig. 3. The microwave power is supplied from a magnetron generator [CEFEMO 2M240H(Y) magnetron head equipped with DIPOLAR Magdrive1000 high voltage power supply and ferrite isolator] to the MPS via a rectangular waveguide (WR 340 standard) equipped with a calibrated directional coupler and 3-stub tuner. The directional coupler makes it possible to measure the power of incident (P_I) and reflected (P_R) microwaves, and thus the microwave power supplied to the MPS ($P_A = P_I - P_R$). The 3-stub tuner (a kind of matching circuit) allows the power of the reflected microwaves to be minimised, and

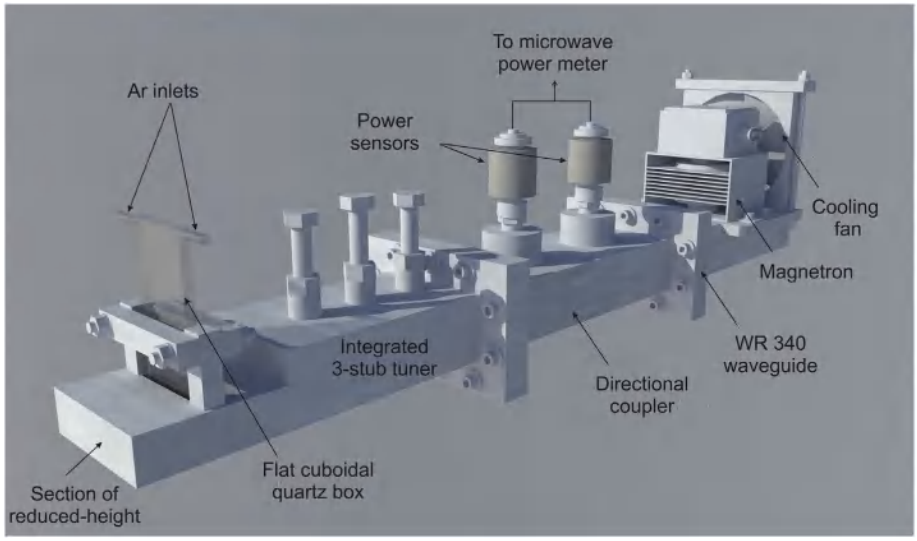

Fig. 2. General scheme of the experimental setup with the MPS for the plasma sheet generation.

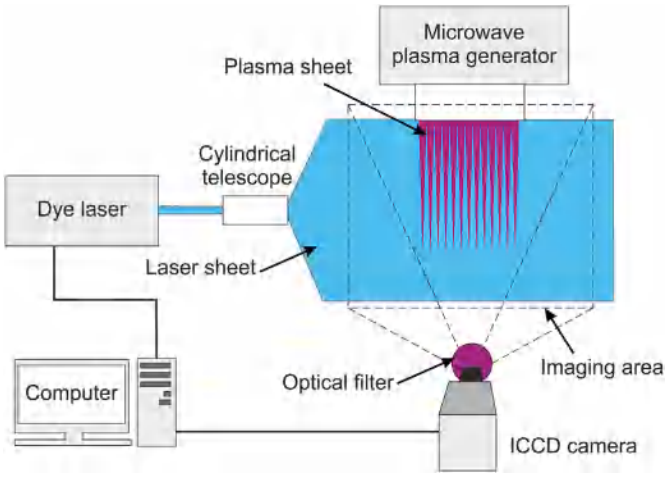

Fig. 4. Diagram of the experimental setup for LIF measurements.

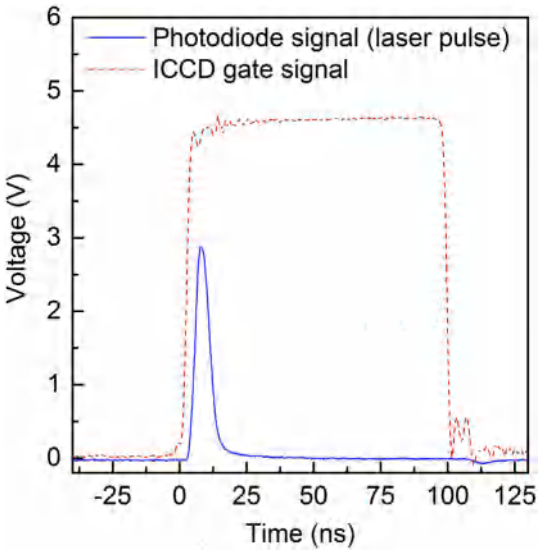

Fig. 5. Laser pulse ($t_i = 10$ ns) and ICCD camera gate signal ($t_g = 100$ ns). Laser pulse was registered using Thorlabs DET10A/M photodiode (raise time of 1 ns).

subsequently, to reduce microwave power loss. The main element of the MPS is a flat cuboidal quartz box to which the working gas (argon) is being supplied. Two argon inlets are introduced into the box through two opposite channels located in its upper part. The inner dimensions, i.e. length, width and thickness are 119 mm, 47 mm and 1 mm, respectively. The box protrudes 2 mm above the wall of the waveguide. Inside the quartz box, a microwave discharge occurs, leading to the formation of a plasma in the form of a sheet. The generated plasma protrudes outside the quartz box. The distance to which the plasma protrudes depends on the microwave power and argon flow rate delivered to the MPS.

During the experimental investigations the presented MPS was operated with an argon flow rate between 10 L min^{-1} and 30 L min^{-1} and with the absorbed microwave power being varied between 300 W and 850 W.

In Fig. 3, a photo of the actual microwave plasma sheet is shown, in which the measuring area of the LIF diagnosis is marked. The visible plasma sheet is generated at an argon flow rate of 20 L/min^{-1} and a microwave power of 850 W delivered to the MPS.

3.2. LIF apparatus for OH measurements

The spatial distribution of the OH radicals in the argon microwave plasma sheet was measured using the LIF method with the experimental setup shown schematically in Fig. 4.

In order to excite the OH radicals in the microwave plasma sheet, a tunable dye laser (Quantel TDL+) with a Rhodamine 590 pumped by the nanosecond Nd:YAG laser (Quantel Q-smart) at $\lambda = 532$ nm was used. The dye laser radiation frequency was doubled using second-harmonic generation resulting in a radiation wavelength of $\lambda = 282.367$ nm tuned to the excitation transition of the OH radicals. The laser pulse energy and width were respectively $E_i = 8.1$ mJ $\pm$ 0.4 mJ and $t_i = 10$ ns. A laser sheet (of thickness of 0.5 mm and height of 30 mm) formed from the laser beam by a cylindrical telescope was introduced into the microwave plasma sheet in such a way that it overlapped with the plasma sheet plane. The power density of laser pulse in plane of plasma formation was $5.4 \cdot 10^6$ W/cm^2. The OH fluorescence radiation ($\lambda = 309$ nm) was recorded using an ICCD (Intensified CCD) camera placed perpendicularly to the laser sheet, as shown in Fig. 4. The ICCD camera was equipped with a narrow bandpass optical filter (FWHM $\lambda = 10$ nm) matched to the wavelength of the OH fluorescence radiation. The time relations of the ICCD camera gate signal fixed at 100 ns and the laser pulse signal are shown in Fig. 5.

4. Results and discussion

The production of OH radicals in the presented microwave discharge is based on the dissociation of water vapour in collisions either with electrons or excited argon atoms [24]:

$$H_2O + e \rightarrow OH + H + e, \quad k = 2.3 \times 10^{-12} - 1.8 \times 10^{-10}\,cm^3 s^{-1},$$

$$H_2O + Ar* \rightarrow OH + H + Ar, \quad k = 2.1 \times 10^{-10}\,cm^3 s^{-1}.$$

The use of argon as the working gas is vital, mainly for two reasons. Firstly, the properties of argon, in contrast to molecular gases, allow a convenient plasma shape in the form of a sheet to be obtained at a relatively low microwave power level (~300÷850 W). Secondly, argon plasma has a relatively low temperature (~800÷1000 K), which is an

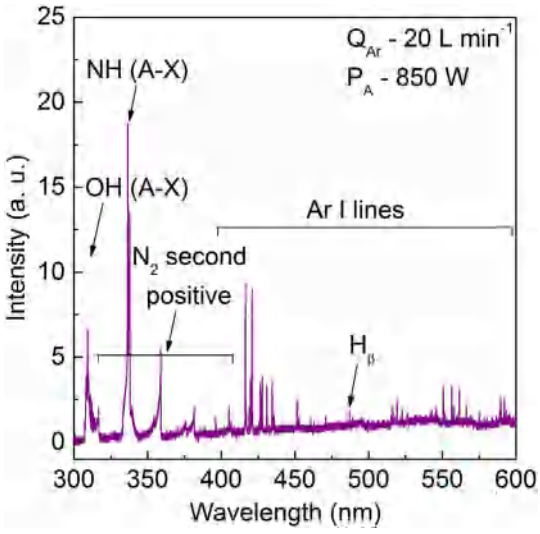

Fig. 6. Emission spectrum of microwave plasma sheet discharge. Microwave power: 850 W, Argon flow rate: 20 L/min^{-1}.

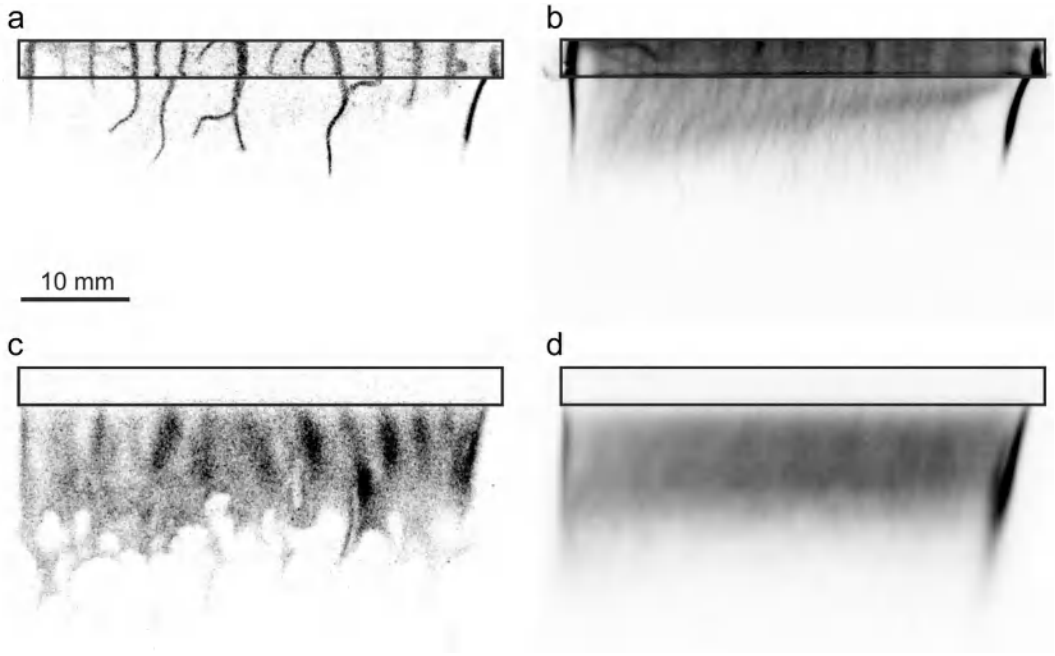

Fig. 7. a) Direct emission single image (ICCD gate: 100 ns, no filter), b) Direct emission averaged image (over 100 single images), c) LIF single image (ICCD gate: 100 ns, 309 nm narrowband filter), d) LIF averaged image (over 100 single images). Light intensity in direct emission and LIF images is not to scale. Microwave power: 620 W, Argon flow rate: 20 L/min^{-1}, LIF laser pulse energy: 8,0 mJ, laser wavelength: 282,372, laser pulse repetition rate: 10 Hz. Black rectangle - nozzle.

advantage for the functioning and life of the device. The plasma sheet contains many filaments characteristic of microwave argon plasmas generated at atmospheric pressure. The phenomenon of filamentation is not yet fully understood, but its causes can be attributable to the skin effect and the low thermal conductivity of argon [25]. The skin effect limits the penetration of the microwave electric field into the plasma, and thus determines the upper limit of the filament's radius. The low thermal conductivity of the gas induces fast radial changes in the gas temperature in the plasma.

The presence of the OH radicals in the discharge can be confirmed by emission spectroscopy. In Fig. 6, the typical emission spectra are presented where the OH emission is visible around 310 nm. However, only the excited molecules can be detected by emission spectroscopy. To obtain information about the distribution of OH in a ground state, the planar LIF method was applied. In this experiment, we studied the relative concentration of the OH radicals as a function of microwave power and argon flow rate. Using the LIF method, we can also study the temporal decay of the OH radicals in the microwave plasma.

We captured the fast gated images (gate time was 100 ns) of the microwave plasma sheet by means of a traditional direct emission imaging method. The fast gated images indicate that the plasma sheet is composed of individual plasma filaments (Fig. 7a) with a diameter of approximately 0.5 mm and a length of 10 mm. We observed that individual plasma filaments can branch into two filaments. It was found that the plasma filaments appear in random places on the plasma sheet. Fig. 7b shows an averaged image of the plasma sheet composed of 100 summarised fast gated images. The slight asymmetry of the plasma intensity in the horizontal direction seen in Fig. 7b is the effect of the non-uniform gas flow in the quartz box. A single LIF image showing the spatial distribution of the OH radicals in the plasma sheet, and a LIF image averaged over 100 individual single LIF images are presented in Fig. 7c and d, respectively. Fig. 7c reveals that the OH radicals are produced uniformly in the whole plasma sheet and not only in the close proximity of the plasma filaments. The length of the OH production area is about 10 mm and is similar to the length of the plasma filaments. The averaged OH image (Fig. 7d) shows the asymmetry in the OH relative concentration due to nonuniformity in the gas flow, similar to that observed in the plasma sheet (Fig. 7b).

In Fig. 8, the temporal behavior of the LIF OH signal is presented. The data presented in the plot was averaged over 30 measurements. Fig. 8 shows that the LIF signal decreases exponentially with elapsing time and within 200 ns the LIF signal decreases to about 5% of its maximal intensity (measured for time delay of 0 ns). We have found that for times longer than 200 ns the intensity of the LIF signal approached the sensitivity limit of the ICCD camera limiting the practical measuring time window to about 200 ns.

The LIF OH signal from the microwave discharge with an argon flow rate of 10, 20 and 30 L min^{-1} as a function of microwave power is

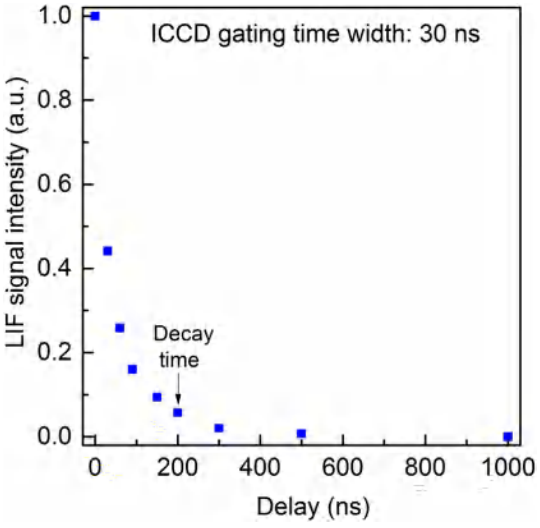

Fig. 8. Normalized LIF signal intensity as the function of ICCD gating time delay in respect to the laser pulse. ICCD gating time width: 30 ns.

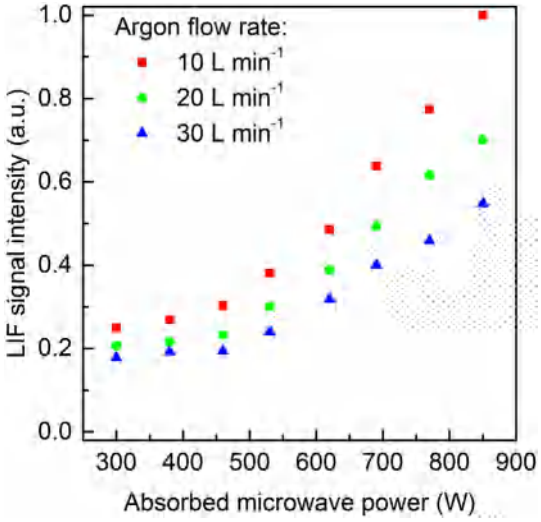

Fig. 9. Normalized LIF signal intensity as the function of microwave power for three values of argon flow rate. ICCD gating time width: 100 ns.

shown in Fig. 9. The data was averaged from over 100 measurements. As seen in the figure, the LIF OH signal from the microwave discharge, thus the relative concentration of the OH radicals, increased with increasing microwave power delivered to the MPS. This increase could be explained by the increase of the electric field in the plasma region with the increasing microwave power. The higher electric field is the cause of the increase in the number and the energy of electrons leading to the increased number of OH radicals generated in collisions between the water vapour molecules and the energetic electrons and excited argon atoms. Increasing the argon flow rate at constant microwave power resulted in reducing the residence time of the gaseous species in the plasma region, thus as can also be seen in Fig. 9, increasing the argon flow rate resulted in lower values of the relative concentration of the OH radicals.

5. Summary

This paper presents the relative concentration and spatial distribution of OH radicals in a new kind of plasma, i.e. a microwave plasma sheet generated in atmospheric pressure argon, measured by means of the LIF method. It was found that the relative concentration of the OH radicals increases with the increase in microwave power and decreases with the increasing argon flow rate. The LIF OH images suggest that the OH generation occurs mainly in the filaments of microwave discharge. However, thanks to the random distribution of the filaments in the discharge, the resulting OH distribution in the steady state is quite uniform.

Acknowledgment

This research was supported by the National Science Centre of Poland, under the project no. 2015/19/B/ST8/02123 and partially by the Institute of Fluid Flow Machinery, Polish Academy of Sciences under the program IMP PAN O3Z1T1.

References

[1] Jasiński M., Goch M., Mizeraczyk J. (2013). Urządzenie plazmowe do obróbki powierzchni elementów (Plasma device for treatment of material surfaces). Patent PL 215139 B1.
[2] H. Nowakowska, D. Czylkowski, B. Hrycak, M. Jasinski, Characterization of a novel microwave plasma sheet source operated at atmospheric pressure, Plasma Sources Sci. Technol. 27 (2018) 085008 , (16 pp) https://doi.org/10.1088/1361-6595/aad402.
[3] H. Conrads, M. Schmidt, Plasma generation and plasma sources, Plasma Sources Sci. Technol. 9 (2000) 441–454, https://doi.org/10.1088/0963-0252/9/4/301.
[4] P. Bruggeman, T. Verreycken, M.Á. González, J.L. Walsh, M.G. Kong, C. Leys, D.C. Schram, Optical emission spectroscopy as a diagnostic for plasma in liquids: opportunities and pitfalls, J. Phys. D. Appl. Phys. 43 (8pp) (2010), 124005. https://doi.org/10.1088/0022-3727/43/12/124005.
[5] A. Sarani, A.Y. Nikiforov, C. Leys, Atmospheric pressure plasma jet in Ar and Ar/H_2O mixtures: optical emission spectroscopy and temperature measurements, Phys. Plasmas 17 (2010), 063504. https://doi.org/10.1063/1.3439685.
[6] C. Miron, M.A. Bratescu, N. Saito, O. Takai, Optical diagnostic of bipolar electrical discharges in HCl, KCl, and KOH solutions, J. Appl. Phys. 109 (2011), 123301. https://doi.org/10.1063/1.3597790.
[7] P. Bruggeman, G. Cunge, N. Sadeghi, Absolute OH density measurement by broadband UV absorption in diffuse atmospheric-pressure He-H_2O RF glow discharges, Plasma Sources Sci. Technol. 21 (0) (2012), 35019 , (7pp) https://doi.org/10.1088/0963-0252/21/3/035019.
[8] G. Dilecce, P.F. Ambrico, M. Simek, S. De Benedictis, OH density measurement by time-resolved broad band absorption spectroscopy in an Ar-H_2O dielectric barrier discharge, J. Phys. D. Appl. Phys. 45 (2012) 125203 , (6pp) https://doi.org/10.1088/0022-3727/45/12/125203.
[9] R. Ono, T. Oda, Dynamics and density estimation of hydroxyl radicals in a pulsed corona discharge, J. Phys. D. Appl. Phys. 35 (2002) 2133–2138, https://doi.org/10.1088/0022-3727/35/17/309.
[10] S. Kanazawa, H. Kawano, S. Watanabe, T. Furuki, S. Akamine, R. Ichiki, T. Ohkubo, M. Kocik, J. Mizeraczyk, Observation of OH radicals produced by pulsed discharges on the surface of a liquid, Plasma Sources Sci. Technol. 20 (2011), 034010. https://doi.org/10.1088/0963-0252/20/3/034010.
[11] S.R. Plimpton, M. Gołkowski, D.G. Mitchell, C. Austin, S.S. Eaton, G.R. Eaton, C. Gołkowski, M. Voskuil, Remote delivery of hydroxyl radicals via secondary chemistry of a nonthermal plasma effluent, Biotechnol. Bioeng. 110 (2013) 1936–1944, https://doi.org/10.1002/bit.24853.
[12] Y. Gorbanev, D. O'Connell, V. Chechik, Ion-thermal plasma in contact with water: the origin of species, Chem. Eur. J. 22 (2016) 3496–3505, https://doi.org/10.1002/chem.201503771.
[13] K. Nagato, Ion species generated by discharge in air and chemical reaction processes, J. Insti. Electrostatics Japan 35 (2011) 102–107.
[14] S. Kanazawa, F. Furuki, T. Nakaji, S. Akamine, R. Ichiki, Measurement of OH radicals in aqueous solution produced by atmospheric-pressure LF plasma jet, Int. J. Plasma Environ. Sci. Technol. 6 (2012) 166–171.
[15] K. Hirano, T. Kobayashi, Coumarin fluorometry to quantitatively detectable OH radicals in ultrasound aqueous medium, Ultrason. Sonochem. 30 (2016) 18–27, https://doi.org/10.1016/j.ultsonch.2015.11.020.
[16] T. Kawasaki, S. Kusumegi, A. Kudo, T. Sakanoshita, T. Tsurumaru, A. Sato, G. Uchida, K. Koga, M. Shiratani, Effects of irradiation distance on supply of reactive oxygen species to the bottom of a Petri dish filled with liquid by an atmospheric O_2/He plasma jet, J. Appl. Phys. 119 (2016), 173301. https://doi.org/10.1063/1.4948430.
[17] R. Ono, T. Oda, Measurement of hydroxyl radicals in an atmospheric pressure discharge plasma by using laser-induced fluorescence, IEEE Trans. Ind. Appl. 36 (2000) 82–86, https://doi.org/10.1109/IAS.1998.729813.
[18] L. Li, A. Nikiforov, Q. Xiong, N. Britun, R. Snyders, X. Lu, C. Leys, OH radicals distribution in an Ar-H_2O atmospheric plasma jet, Phys. Plasmas 20 (2013), 093502. https://doi.org/10.1063/1.4820945.
[19] T. Verreycken, R. Mensink, R.M. van der Horst, N. Sadeghi, P. Bruggeman, Absolute OH density measurements in the effluent of a cold atmospheric-pressure Ar–H_2O RF plasma jet in air, Plasma Sources Sci. Technol. 22 (2013) 055014, https://doi.org/10.1088/0963-0252/22/5/055014.
[20] T. Verreycken, R.M. van der Horst, A.H.F.M. Baede, E.M. van Veldhuizen, P.J. Bruggeman, Time and spatially resolved LIF of OH in a plasma filament in atmospheric pressure He–H_2O, J. Phys. D. Appl. Phys. 45 (2012), 045205 , 8pp https://doi.org/10.1088/0022-3727/45/4/045205.
[21] S. Kanazawa, H. Tanaka, A. Kajiwara, T. Ohkubo, Y. Nomoto, M. Kocik, J. Mizeraczyk, J.-S. Chang, LIF imaging of OH radicals in DC positive streamer coronas, Thin Solid Films 515 (2007) 4266–4271, https://doi.org/10.1016/j.tsf.2006.02.046.
[22] C.C. Wang, L.I. Davis Jr., C.H. Wu, S. Japar, Laser-induced dissociation of ozone and resonance fluorescence of OH in ambient air, Appl. Phys. Lett. 28 (1976) 14–16, https://doi.org/10.1063/1.88561.
[23] M. Kocik, J. Mizeraczyk, S. Kanazawa, A. Kajiwara, J. Kumagai, T. Ohkubo, Y. Nomoto, J.-S. Chang, Observation of ground-state OH by LIF technique in DC nozzle-to-plate positive streamer coronas, Conference Record of the 2004 IEEE Industry Applications Conference, 2004. 39th IAS Annual Meeting 2004, pp. 244–249, https://doi.org/10.1109/IAS.2004.1348416.
[24] P. Bruggeman, D.C. Schram, On OH production in water containing atmospheric pressure plasmas, Plasma Sources Sci. Technol. 19 (4) (2010), 045025. https://doi.org/10.1088/0963-0252/19/4/045025.
[25] Y. Kabouzi, M.D. Calzada, M. Moisan, K.C. Tran, C. Trassy, Radial contraction of microwave-sustained plasma columns at atmospheric pressure, J. Appl. Phys. 91 (2002) 1008–1019, https://doi.org/10.1063/1.1425078.